Nanotechnology Perceptions
ISSN 1660-6795
www.nano-ntp.com

Heat and Mass Transfer Performance of Dufour and Heat Source on Casson Fluid Flow Past an Inclined Oscillating Rotating Porous Plate with Chemical Reactions and Thermal Radiation

C. Manigandan[1] **andS. Senthamilselvi**[2,*]
[1]*Research Scholar, Department of Mathematics, Vels Institute of Science, Technology & Advanced Studies, Chennai-600117, Tamil Nadu, India*
Email: maninaac2021@gmail.com
[2]*Department of Mathematics, Vels Institute of Science, Technology & Advanced Studies. Chennai-600117, Tamil Nadu, India*
[*]*Corresponding author Email: msselvi2305@gmail.com*

Abstract: The current research presents an analytical interpretation of unsteady-free convective hydromagnetic boundary layers, focusing on how the Dufour effect, thermal radiation, and chemical reactions influence Casson fluid flow through a rotating porous medium, around an inclined oscillating platewithin a uniformfield. The governing equations are solved using the Laplace transform method, with the results presented visually through numerical values of Casson fluid velocity, temperature, and concentration at the plate, based on various key parameter values. The study examines how the Casson fluid behaves compared to Newtonian fluid, with the Casson fluid demonstrating a higher velocity. The findings also show that, as temperature decreases, parameters such as the Grashof number, Dufour effect, thermal radiation parameter (R), and chemical reaction parameter (K) increase. Additionally, increasing the chemical reaction parameter (K) causes a reduction in concentration. In analyzing the fluid flow, the study also measured the influence of Prandtl, Schmidt, thermal, and Grashof numbers. The results indicate that the velocity of the fluid decreases with higher radiation levels, but increases when the heat source and Grashof number are elevated. Similarly, rising radiation levels reduce temperature, while a stronger heat source increases it.
Keywords: Dufour, Heat source, Thermal Radiation, Chemical Reaction, Rotation

1. Introduction

The study of radiative heat and mass transport in convective flows is relevant for many industrial and technical applications. Mass transfer is a prevalent phenomenon in the chemical industry, as well as the physical and biological sciences.Heat transfer in porous media from different geometries has many scientific and practical applications, such as geothermal reservoirs, drying of porous solids, thermal insulation, enhanced oil recovery, packed-bed catalytic reactors, nuclear reactor cooling, and underground energy

transfer. Current research in radiative heat transfer heavily focuses on numerical simulations of coupled radiation and convection processes. Convective heat transfer in porous media has recently gained significant attention due to its technological relevance in several domains. For example, Muthucumaraswamyet al. [1] studied Radiative Flow Past a Parabolic Started Isothermal Vertical Plate with Uniform Mass Flux.A.K. Agrawalet a. [2] examined free convection due to thermal and mass diffusion in laminar flow of an accelerated infinite vertical plate in the presence of magnetic. Kataria et al. [3] explored the impact of radiation and chemical reactions on the flow of MHD Casson fluid over a vertical oscillating plate in a porous medium.

Vijayaragavan et al. [4] provided a theoretical solution to the problem of heat and mass transfer in MHD Casson fluid flow past a sloped porous plate with Dufour and chemical reactions. Kavitha et al. [5] investigated parabolic flow over a rotating isothermal plate with uniform temperature and mass diffusion in the presence of a chemical reaction. Selvaraj et al. [6] explored MHD parabolic flow over a rotating, accelerating isothermal plate, while Nanadakumar et al. [7] studied the combined Soret and MHD effects on parabolic flow past a quickly moving vertical plate.Jothi and Selvaraj [8] examined the impact of a heat source on MHD flow and a radiation-absorbing fluid moving over an exponentially accelerating plate surrounded by a porous medium. According to Lakshmikaanth et al. [9], as radiation (R) increases, the temperature decreases, whereas an increase in the heat source (Q) raises the temperature. Maran [10] and his team studied mass and heat transfer over a vertical plate during chemical reactions and thermal diffusion, where MHD effects did not govern the convective flow.Aruna et al. [11] explored the Hall and magnetic effects on a fluid flowing past a parabolically accelerated vertical plate, considering both heat variations and uniform mass diffusion due to thermal radiation. Radha et al. [12] discussed the MHD effects on Casson fluid flow over a parabolically accelerated vertical plate with thermal diffusion in unsteady conditions. Muthucumaraswamy Rajamanickam et al. [13–14] analyzed free convection in MHD flow past a moving vertical plate with constant temperature during a chemical reaction, also investigating the Hall and rotational effects on heat and mass transfer in magnetohydrodynamic flow over a vertically oriented plate under exponential acceleration.

Hetnarski [15, 16] presented an algorithm for finding inverse Laplace transforms. Sarma and Ahmed [17] studied the Dufour effect in non-steady MHD flow through a porous medium over a vertical plate with rising temperature. Prakash and Selvaraj [18] investigated how radiation and heat impact MHD and parabolic motion in Casson fluids moving through a rotating porous medium on a vertical plate. Prabhakar et al. [19] used computational techniques to explore the effects of diffusion, thermodynamics, and rotation on heat-generating MHD Casson fluid flow past an oscillating porous plate.Ananda Reddy and Janardhan [20] corrected for the Soret and Dufour effects on MHD Casson fluid over a vertical plate in the presence of chemical reactions and radiation. Palani and Arutchelvi [21] analyzed the flow of an MHD nanofluid past an inclined plate, accounting for the Soret and Dufour effects. Kumar and Vempati [22, 23] studied the influence of MHD on the rapid starting of an infinite vertical plate under temperature variations in a horizontal magnetic field. MuthucumaraswamyRajamanickan et al. [24, 25] examined chemical reaction effects on flow past a vertical plate undergoing rapid motion with varying temperatures and mass diffusion in the presence of a magnetic field.Patel and Harshad R. [26] investigated cross-

diffusion and heat generation effects on mixed convective MHD flow of Casson fluid through a porous medium with non-linear thermal radiation. Dhanalakshmi et al. [27] discussed molecular stability, kinetic energy, and energy-related factors in coumarin compounds through Gc-MS analysis. Karthikeyan et al. [28, 29] explored the rotational effects of parabolic flow past an isothermal vertical plate using MHD, while Gayathri et al. [30] studied the Soret and Dufour effects on unsteady MHD convective flow over an infinite vertical porous plate.In this study, we investigated the Dufour effects on MHD Casson fluid flow past an exponentially accelerating inclined oscillating plate, in comparison to a rotating fluid with constant temperature and mass diffusion

2. Mathematical Formulation

Consider an unsteady free hydromagnetic natural convective flow involving heat and mass transfer in a viscous, incompressible, electrically conductive, and optically thick radiative fluid. The fluid flows past an infinite inclined oscillating plate within a rotating system. The model incorporates the effects of the Hall current, rotation, and the presence of a porous medium, while also accounting for the Dufour effect. The coordinate system is chosen such that$y'-$ axis is perpendicular to the plate and $x'-$ axis is upward to the plate. The plate and fluid revolve along $x'-$ axis in according with standardized angular velocity Ω .The fluid and plate initially rest at period along $t' \leq 0$ and are held at the uniform temperature T'. Also, on the surface of the plate, and at any point inside the fluid, species concentration at $\mathrm{C'}_{\infty}$ shall be preserved uniformly. At the time$t' \geq 0$, plate statistics moving to their own planes at $u' = u_0 cos wt$ velocity.The flow temperature and species concentration on the plate surface is upturned to the uniform temperature about T'_{w} and uniform species concentration C'_{w} and consequently retained.

Under these conditions, the flow characteristics solely depend on y' and t Plate temp is decreased or increased to $\mathrm{T'}_{\infty} + (\mathrm{T'}_{w} - \mathrm{T'}_{\infty})\frac{{u_0}^2 \bar{t}}{v}$ at $\bar{t} \geq 0$ and plate concentration is raised or lowered to $\mathrm{C'}_{\infty} + (\mathrm{C'}_{w} - \mathrm{C'}_{\infty})\frac{{u_0}^2 \bar{t}}{v}$ at $\bar{t} \geq 0$. The rheological state eq. for Cauchy stress tensor of Casson fluid is presented by

$$\tau_{ij} = \begin{cases} 2e_{ij}\left(\mu_B + \frac{py}{\sqrt{2\pi}}\right) & \pi > \pi_c \\ 2e_{ij}\left(\mu_B + \frac{py}{\sqrt{2\pi_c}}\right) & \pi < \pi_c \end{cases}$$

$$\frac{\partial \mathrm{u}'}{\partial \mathrm{t}'} - 2\Omega'\mathrm{v}' = \vartheta\left(1 + \frac{1}{\gamma}\right)\frac{\partial^2 \mathrm{u}'}{\partial \mathrm{y}'^2} + \mathrm{g}\beta_{\mathrm{T}'}(\mathrm{T}' - \mathrm{T'}_{\infty})\cos\alpha + \mathrm{g}\beta_{\mathrm{C}'}(\mathrm{C}' - \mathrm{C}'_{\infty})\cos\alpha - \frac{\vartheta \mathrm{u}'}{k_1'} \quad (1)$$

$$\frac{\partial \mathrm{v}'}{\partial \mathrm{t}'} + 2\Omega'\mathrm{u}' = \vartheta\frac{\partial^2 \mathrm{v}'}{\partial \mathrm{y}'^2} - \frac{\vartheta u'}{k_1'} \quad (2)$$

$$\frac{\partial \theta'}{\partial t'} = \frac{k}{\rho C_p}\frac{\partial^2 \theta'}{\partial y'^2} - \frac{1}{\rho C_p}\frac{\partial q_r'}{\partial y'} + \frac{Q_0}{\rho C_p}(\mathrm{T}' - \mathrm{T'}_{\infty})' + \frac{D_m K_T}{C_s C_p}\frac{\partial^2 C'}{\partial y'^2} \quad (3)$$

$$\frac{\partial \mathrm{C}'}{\partial \mathrm{t}'} = \frac{1}{S_c}\frac{\partial^2 \mathrm{C}'}{\partial \mathrm{y}'^2} - \mathrm{k}'(\mathrm{C}' - \mathrm{C}'_{\infty}) \quad (4)$$

The initial and boundary conditions listed below

$$\left.\begin{array}{c} \mathrm{u}' = 0, \mathrm{v}' = 0\,, \mathrm{T}' = \mathrm{T'}_{\infty},\ \mathrm{C}' = \mathrm{C}'_{\infty},\ \text{for all } \mathrm{z}' \geq 0\,, \mathrm{t}' \leq 0 \\ \mathrm{u}' = u_0 cos wt, \quad \mathrm{T}' = \mathrm{T'}_{\infty} + (\mathrm{T}'_{\mathrm{w}} - \mathrm{T'}_{\infty})\frac{\mathrm{t}'}{t_0}, C' = (\mathrm{C}'_{\mathrm{w}} - \mathrm{C}'_{\infty})\frac{\mathrm{t}'}{t_0} \\ \mathrm{u}' \to 0, \quad \mathrm{T}' \to \mathrm{T}'_{\infty},\ \mathrm{C}' \to \mathrm{C}'_{\infty}\ \text{as}\ \mathrm{z}' \to \infty \text{ and } \mathrm{t}' \geq 0 \end{array}\right\} (5)$$

As we have optically thick Casson fluid, we can use Rosseland approximation [26]

$$\frac{\partial q_r}{\partial z'} = -4a^*\sigma(T'^4_\infty - T'^4) \quad (6)$$

It is assumed that the temperature variations within the flow are small enough T'^4 that can be approximated as a linear function of temperature. This is achieved by expanding T'^4 in a Taylor series around T'_∞ T∞ and neglecting higher-order terms. Thus, the expression becomes

$$T'^4 \cong 4T'^3_\infty T' - 3T'^4_\infty \quad (7)$$

The consequent dimensionless aggregate is

$$\left.\begin{gathered} U = \frac{u'}{U_0},\ V = \frac{v'}{U_0},\ t = \frac{t'}{t_0},\ y = \frac{y'}{U_0 t_0}, \gamma = \frac{\mu_{B\sqrt{2\pi_c}}}{P_y} \\ \theta = \frac{T'-T'_\infty}{T'_w-T'_\infty}, G_r = \frac{g\beta(T'_w-T'_\infty)}{u_0}, C = \frac{C'-C'_\infty}{C'_w-C'_\infty}, G_C = \frac{g\beta(C'-C'_\infty)}{C'_w-C'_\infty}\ ,\ Q = \frac{Q_0 v^2}{kU_0^2} \\ P_r = \frac{\mu C_p}{k}\ ,\ K = \frac{vk_1}{U_0^2},\ S_c = \frac{v}{D}\ , R = \frac{16a^*\sigma T'^3_\infty}{kU_0^2} \end{gathered}\right\} \quad (8)$$

By substituting the values from Eq. (6) and Eq. (7) into Eq. (3), as well as into Eqs. (1)–(4), and simplifying by dropping the notation (for clarity), we obtain the following non-dimensional equations:

$$\frac{\partial U}{\partial t} = \left(1+\frac{1}{\gamma}\right)\frac{\partial^2 U}{\partial y^2} + 2\Omega v + Gr\theta(cos\alpha) + GcC(cos\alpha) - \frac{U}{k_1} \quad (9)$$

$$\frac{\partial V}{\partial t} = \left(1+\frac{1}{\gamma}\right)\frac{\partial^2 V}{\partial y^2} - 2\Omega v - \frac{V}{k_1} \quad (10)$$

$$\frac{\partial \theta}{\partial t} = \frac{1}{P_r}\frac{\partial^2 \theta}{\partial y^2} - R\theta + Q\theta + Df\frac{\partial^2 C}{\partial z^2} \quad (11)$$

$$\frac{\partial C}{\partial t} = \frac{1}{S_c}\frac{\partial^2 C}{\partial y^2} - KC \quad (12)$$

To solve equations (1) and (2), use $q' = U + iV$ we get

$$\frac{\partial q'}{\partial t} = G_r\theta cos(\alpha) + G_C C\cos(\alpha) + \left(1+\frac{1}{\gamma}\right)\frac{\partial^2 q}{\partial y^2} - m^* q' \quad (13)$$

$$\frac{\partial \theta}{\partial t} = \frac{1}{P_r}\frac{\partial^2 \theta}{\partial y^2} - R\theta + Q\theta + Df\frac{\partial^2 C}{\partial y^2} \quad (14)$$

$$\frac{\partial \mathrm{C}}{\partial \mathrm{t}} = \frac{1}{\mathrm{S_c}}\frac{\partial^2 \mathrm{C}}{\partial y^2} - \mathrm{KC} \quad (15)$$

Here $m^* = 2\left[i\Omega + \frac{1}{k_1}\right]$

The corresponding initial and boundary conditions are

$$\left.\begin{gathered} q' = 0, \theta = 0, C = 0\ for\ all\ y\ and\ t \le 0 \\ q' = coswt, \theta = 1\ , C = 1\ \ for\ all\ y\ , t \ge 0 \\ \mathrm{q'} \to 0, \theta \to 0, C \to 0\ as\ y \to \infty. \end{gathered}\right\} \quad (16)$$

3. Solution of the Problem

The dimensionless governing equations (14), (15), and (16), along with their initial and boundary conditions, can be solved using the Laplace transform technique we get the solutions

$$C = \frac{1}{2}\left[e^{-2\eta\sqrt{ScKt}}\ erfc\left(\eta\sqrt{Sc} - \sqrt{Kt}\right) + e^{2\eta\sqrt{ScKt}}\ erfc\left(\eta\sqrt{Sc} + \sqrt{Kt}\right)\right] \quad (17)$$

$$\theta = \theta_1 + \frac{P_r D_f S_c}{(S_c - P_r)}\left(\frac{a+K}{a}\right)[\theta_2 + \theta_3] + \frac{P_r D_f S_c}{(S_c - P_r)}\frac{K}{a}[\theta_5 + \theta_6] \quad (18)$$

Where $\theta_1 = \frac{1}{2}\begin{bmatrix} e^{-2\eta\sqrt{P_r(R-Q)t}}\, erfc\left(\eta\sqrt{Pr} - \sqrt{(R-Q)t}\right) \\ +e^{2\eta\sqrt{P_r(R-Q)t}}\, erfc\left(\eta\sqrt{Pr} + \sqrt{(R-Q)t}\right) \end{bmatrix}$

$$\theta_2 = \frac{e^{at}}{2}\begin{bmatrix} e^{-2\eta\sqrt{P_r(a+R-Q)t}}\, erfc\left(\eta\sqrt{Pr} - \sqrt{(a+R-Q)t}\right) \\ +e^{2\eta\sqrt{P_r(a+R-Q)t}}\, erfc\eta\sqrt{Pr} + \sqrt{(a+R-Q)t} \end{bmatrix}$$

$$\theta_3 = \frac{e^{at}}{2}\begin{bmatrix} e^{-2\eta\sqrt{S_c(a+K)t}}\, erfc\left(\eta\sqrt{S_c} - \sqrt{(a+K)t}\right) \\ +e^{2\eta\sqrt{S_c(a+K)t}}\, erfc\left(\eta\sqrt{S_c} + \sqrt{(a+K)t}\right) \end{bmatrix}$$

$$\theta_4 = \frac{1}{2}\left[e^{-2\eta\sqrt{S_c K t}}\, erfc\left(\eta\sqrt{S_c} - \sqrt{Kt}\right) + e^{2\eta\sqrt{S_c K t}}\, erfc\left(\eta\sqrt{S_c} + \sqrt{Kt}\right)\right]$$

$$\theta_5 = \frac{1}{2}\begin{bmatrix} e^{-2\eta\sqrt{P_r(R-Q)t}}\, erfc\left(\eta\sqrt{Pr} - \sqrt{(R-Q)t}\right) \\ +e^{2\eta\sqrt{P_r(R-Q)t}}\, erfc\eta\sqrt{Pr} + \sqrt{(R-Q)t} \end{bmatrix}$$

q'

$$= f_1 + f_2$$

$$+\frac{Gr(cos\alpha)}{a_1}\begin{bmatrix} f_3 - f_4 + \frac{PrDfSc}{Sc-Pr}\left(\frac{k+a}{a}\right)\left\{\frac{1}{a-c_1}(f_5 - f_6 - f_7 + f_8) - \frac{1}{a-d}(f_9 - f_{10} - f_{11} + f_{12})\right\} \\ + \\ \frac{PrDfSc}{Sc-Pr}\left(\frac{k}{a}\right)\left\{\frac{1}{d}(-f_{13} + f_{14} + f_{15} - f_{16}) - \frac{1}{c_1}(-f_{17} + f_{18} + f_{19} - f_{20})\right\} \end{bmatrix}$$

$$+\frac{Gc(cos\alpha)}{a_1 b}[f_{21} - f_{22} - f_{23} + f_{24}] \quad (19)$$

where

$$f_1 = \begin{bmatrix} e^{-2\eta\sqrt{\frac{(m^*-iw)t}{a_1}}}\, erfc\left(\frac{\eta}{\sqrt{a_1}} - \sqrt{(m^*-iw)t}\right) \\ +e^{2\eta\sqrt{\frac{(m^*-iw)t}{a_1}}}\, a_1 erfc\left(\frac{\eta}{\sqrt{a_1}} - \sqrt{(m^*-iw)t}\right) \end{bmatrix}$$

$$f_2 = \frac{e^{iwt}}{4}\begin{bmatrix} e^{-2\eta\sqrt{\frac{(m^*+iw)t}{a_1}}}\, erfc\left(\frac{\eta}{\sqrt{a_1}} - \sqrt{(m^*+iw)t}\right) \\ +e^{2\eta\sqrt{\frac{(m^*-iw)t}{a_1}}}\, erfc\left(\frac{\eta}{\sqrt{a_1}} + \sqrt{(m^*+iw)t}\right) \end{bmatrix}$$

$$f_3 = \frac{e^{c_1 t}}{2}\left[e^{-2\eta\sqrt{\frac{(m^*+c_1)t}{a_1}}} erfc\left(\eta - \sqrt{\frac{(m^*+c_1)t}{a_1}}\right) + e^{2\eta\sqrt{\frac{(m^*+c_1)t}{a_1}}} erfc\left(\eta + \sqrt{\frac{(m^*+c_1)t}{a_1}}\right)\right]$$

$$f_4 = \frac{e^{c_1 t}}{2}\left[\begin{matrix} e^{-2\eta\sqrt{Pr(R+c_1-Q)t}} erfc\left(\eta\sqrt{Pr} - \sqrt{(R+c_1-Q)t}\right) \\ +e^{2\eta\sqrt{Pr(R+c_1-Q)t}} erfc\left(\eta\sqrt{Pr} + \sqrt{(R+c_1-Q)t}\right)\end{matrix}\right]$$

$$f_5 = \frac{e^{at}}{2}\left[e^{-2\eta\sqrt{\frac{(m^*+a)t}{a_1}}} erfc\left(\eta - \sqrt{\frac{(m^*+a)t}{a_1}}\right) + e^{2\eta\sqrt{\frac{(m^*+a)t}{a_1}}} erfc\left(\eta + \sqrt{\frac{(m^*+a)t}{a_1}}\right)\right]$$

$$f_6 = \frac{e^{c_1 t}}{2}\left[e^{-2\eta\sqrt{\frac{(m^*+c_1)t}{a_1}}} erfc\left(\eta - \sqrt{\frac{(m^*+c_1)t}{a_1}}\right) + e^{2\eta\sqrt{\frac{(m^*+c_1)t}{a_1}}} erfc\left(\eta + \sqrt{\frac{(m^*+c_1)t}{a_1}}\right)\right]$$

$$f_7 = \frac{e^{at}}{2}\left[\begin{matrix} e^{-2\eta\sqrt{Pr(R+a-Q)t}} erfc\left(\eta\sqrt{Pr} - \sqrt{(R+a-Q)t}\right) \\ +e^{2\eta\sqrt{Pr(R+a-Q)t}} erfc\left(\eta\sqrt{Pr} + \sqrt{(R+a-Q)t}\right)\end{matrix}\right]$$

$$f_8 = \frac{e^{c_1 t}}{2}\left[\begin{matrix} e^{-2\eta\sqrt{Pr(R+c_1-Q)t}} erfc\left(\eta\sqrt{Pr} - \sqrt{(R+c_1-Q)t}\right) \\ +e^{2\eta\sqrt{Pr(R+c_1-Q)t}} erfc\left(\eta\sqrt{Pr} + \sqrt{(R+c_1-Q)t}\right)\end{matrix}\right]$$

$$f_9 = \frac{e^{at}}{2}\left[e^{-2\eta\sqrt{\frac{(m^*+a)t}{a_1}}} erfc\left(\eta - \sqrt{\frac{(m^*+a)t}{a_1}}\right) + e^{2\eta\sqrt{\frac{(m^*+a)t}{a_1}}} erfc\left(\eta + \sqrt{\frac{(m^*+a)t}{a_1}}\right)\right]$$

$$f_{10} = \frac{e^{dt}}{2}\left[e^{-2\eta\sqrt{\frac{(m^*+d)t}{a_1}}}erfc\left(\eta - \sqrt{\frac{(m^*+d)t}{a_1}}\right) + e^{2\eta\sqrt{\frac{(m^*+d)t}{a_1}}}erfc\left(\eta + \sqrt{\frac{(m^*+d)t}{a_1}}\right)\right]$$

$$f_{11} = \frac{e^{at}}{2}\left[\begin{matrix}e^{-2\eta\sqrt{Sc(a+k)t}}erfc\left(\eta\sqrt{Sc} - \sqrt{(a+k)t}\right)\\ +e^{2\eta\sqrt{Sc(a+k)t}}erfc\left(\eta\sqrt{Sc} + \sqrt{(a+k)t}\right)\end{matrix}\right]$$

$$f_{12} = \frac{e^{dt}}{2}\left[\begin{matrix}e^{-2\eta\sqrt{Sc(d+k)t}}erfc\left(\eta\sqrt{Sc} - \sqrt{(d+k)t}\right)\\ +e^{2\eta\sqrt{Sc(d+k)t}}erfc\left(\eta\sqrt{Sc} + \sqrt{(d+k)t}\right)\end{matrix}\right]$$

$$f_{13} = \frac{1}{2}\left[e^{-2\eta\sqrt{\frac{m^*t}{a_1}}}erfc\left(\eta - \sqrt{\frac{m^*t}{a_1}}\right) + e^{2\eta\sqrt{\frac{m^*t}{a_1}}}erfc\left(\eta + \sqrt{\frac{m^*t}{a_1}}\right)\right]$$

$$f_{14} = \frac{e^{dt}}{2}\left[e^{-2\eta\sqrt{\frac{(m^*+d)t}{a_1}}}erfc\left(\eta - \sqrt{\frac{(m^*+d)t}{a_1}}\right) + e^{2\eta\sqrt{\frac{(m^*+d)t}{a_1}}}erfc\left(\eta + \sqrt{\frac{(m^*+d)t}{a_1}}\right)\right]$$

$$f_{15} = \frac{1}{2}\left[e^{-2\eta\sqrt{Sckt}}erfc\left(\eta\sqrt{Sc} - \sqrt{kt}\right) + e^{2\eta\sqrt{Sckt}}erfc\left(\eta\sqrt{Sc} + \sqrt{kt}\right)\right]$$

$$f_{16} = \frac{e^{dt}}{2}\left[e^{-2\eta\sqrt{Sc(d+k)t}}erfc\left(\eta\sqrt{Sc} - \sqrt{(d+k)t}\right) + e^{2\eta\sqrt{Sc(d+k)t}}erfc\left(\eta\sqrt{Sc} + \sqrt{(d+k)t}\right)\right]$$

$$f_{17} = \frac{1}{2}\left[e^{-2\eta\sqrt{\frac{m^*t}{a_1}}}erfc\left(\eta - \sqrt{\frac{m^*t}{a_1}}\right) + e^{2\eta\sqrt{\frac{m^*t}{a_1}}}erfc\left(\eta + \sqrt{\frac{m^*t}{a_1}}\right)\right]$$

$$f_{18} = \frac{e^{c_1 t}}{2}\left[e^{-2\eta\sqrt{\frac{(m^*+c_1)t}{a_1}}}erfc\left(\eta - \sqrt{\frac{(m^*+c_1)t}{a_1}}\right) + e^{2\eta\sqrt{\frac{(m^*+c_1)t}{a_1}}}erfc\left(\eta + \sqrt{\frac{(m^*+c_1)t}{a_1}}\right)\right]$$

$$f_{19} = \frac{1}{2}\left[\begin{matrix} e^{-2\eta\sqrt{Pr(R-Q)t}}erfc\left(\eta\sqrt{Pr} - \sqrt{(R-Q)t}\right) \\ +e^{2\eta\sqrt{Pr(R-Q)t}}erfc\left(\eta\sqrt{Pr} + \sqrt{(R-Q)t}\right)\end{matrix}\right]$$

$$f_{20} = \frac{e^{c_1 t}}{2}\left[\begin{matrix} e^{-2\eta\sqrt{Pr(R+c_1-Q)t}}erfc\left(\eta\sqrt{Pr} - \sqrt{(R+c_1-Q)t}\right) \\ +e^{2\eta\sqrt{Pr(R+c_1-Q)t}}erfc\left(\eta\sqrt{Pr} + \sqrt{(R+c_1-Q)t}\right)\end{matrix}\right]$$

$$f_{21} = \frac{e^{bt}}{2}\left[e^{-2\eta\sqrt{\frac{(m^*+b)t}{a_1}}}erfc\left(\eta - \sqrt{\frac{(m^*+b)t}{a_1}}\right) + e^{2\eta\sqrt{\frac{(m^*+b)t}{a_1}}}erfc\left(\eta + \sqrt{\frac{(m^*+b)t}{a_1}}\right)\right]$$

$$f_{22} = \frac{1}{2}\left[e^{-2\eta\sqrt{\frac{m^* t}{a_1}}}erfc\left(\eta - \sqrt{\frac{m^* t}{a_1}}\right) + e^{2\eta\sqrt{\frac{m^* t}{a_1}}}erfc\left(\eta + \sqrt{\frac{m^* t}{a_1}}\right)\right]$$

$$f_{23} = \frac{e^{bt}}{2}\left[\begin{matrix} e^{-2\eta\sqrt{Sc(b+k)t}}erfc\left(\eta\sqrt{Sc} - \sqrt{(b+k)t}\right) \\ +e^{2\eta\sqrt{Sc(b+k)t}}erfc\left(\eta\sqrt{Sc} + \sqrt{(b+k)t}\right)\end{matrix}\right]$$

$$f_{24} = \frac{1}{2}\left[e^{-2\eta\sqrt{Sckt}}erfc\left(\eta\sqrt{Sc} - \sqrt{kt}\right) + e^{2\eta\sqrt{Sckt}}erfc\left(\eta\sqrt{Sc} + \sqrt{kt}\right)\right]$$

$$erfc(a+ib) = \mathrm{erf}(a) + \frac{\exp(-a^2)}{2a\pi}[1 - \cos(2ab) + isin(2ab)] + \frac{2\exp(-a^2)}{\pi}\sum_{n=1}^{\infty}\frac{\exp(-\eta^2/4)}{\eta^2 + 4a^2}[f_n(a,b) + ig_n(a,b)] + \in (a,b)$$

Appendix

$$f_n = 2a - 2\,\mathrm{acosh}(nb)\cos(2ab) + n\sinh(nb)\sin(2ab) \quad \text{and}$$

$$g_n = 2\,\mathrm{acosh}(nb)\sin(2ab) + n\sinh(nb)\cos(2ab)$$

$$|\epsilon(a,b)| \approx\approx 10^{-16}|\mathrm{erf}(a+ib)|$$

A=$\left(\frac{Pr(R-Q)-ScK}{Pr-Sc}\right)$, $a_1 = 1 + \frac{1}{\gamma}$,$\eta = \frac{y}{2\sqrt{t}}$ $b = \frac{m^*+KSca_1}{a_1 Sc-1}$,$c = \frac{a_1 Pr(R-Q)}{1-a_1 Pr}$,$d = \frac{ScKa_1-m^*}{1-Sca_1}$,
erfc – Complementary error function

4. Results and Discussions

We are going to look at some numbers that show how different non-dimensional flow parameters affect the speed (q'), temperature (θ), and concentration (C) as they are plotted against the boundary layer coordinate (η) in Fig.1-Fig.16. Chemical reaction parameter (K), rotation parameter (R), Schmidt number (Sc), Grashof number (Gr), Permeability parameter

(k1), Heat absorption coefficient (Q), Dufour number (Df), Casson fluid parameter (γ), and time t.

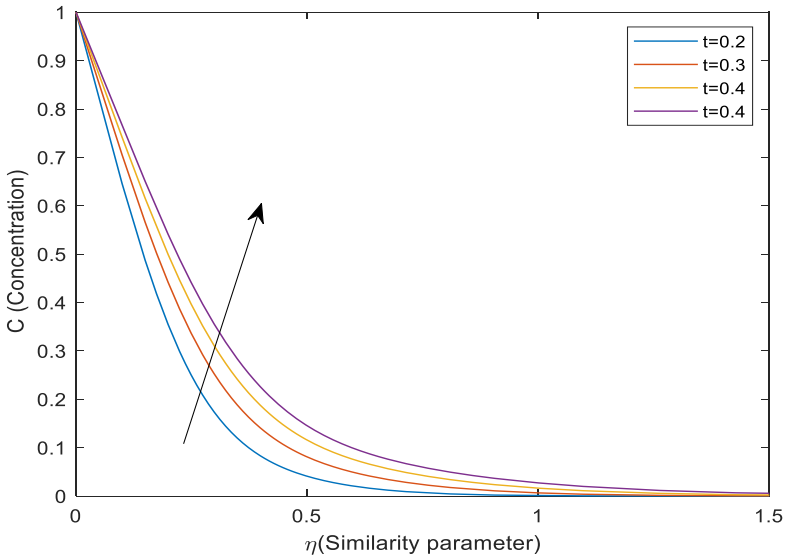

Fig.1 Concentration profile for distinct values of t and Sc=2.01,K=0.5

Fig.1 ,it is observed that the concentration raises with an increase in the value of time t

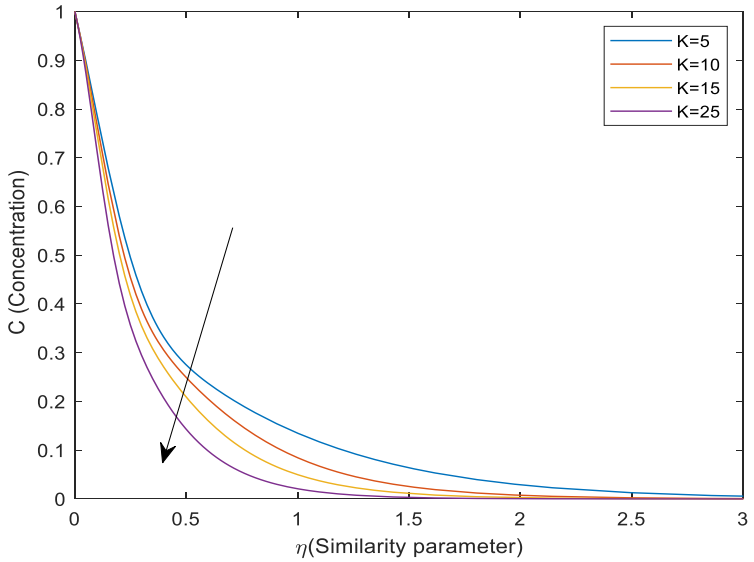

Fig.2 Concentration profile for distinct values of K and time t = 0.2,Sc=2.01

Fig.2 illustrates the concentration goes to down as increase the chemical reaction values

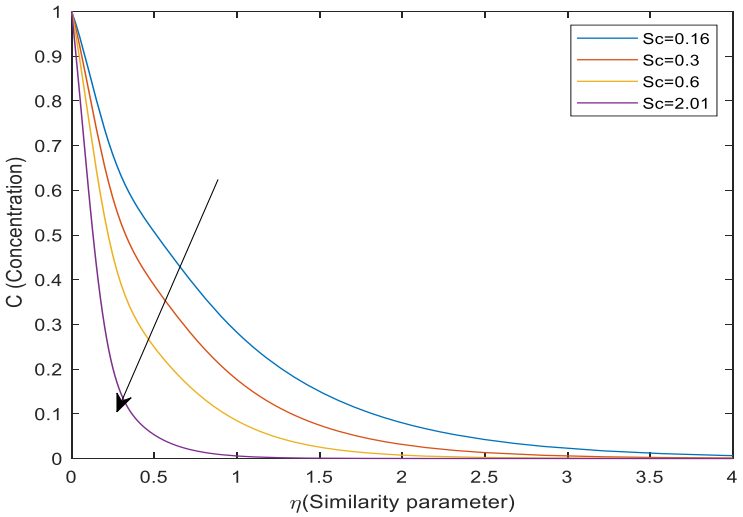

Fig.3 Concentration profile for different value of Sc and values t=0.2,K=10

Using the different values of Schmidt numbers, the result is seen in fig.3 when the Schmidt value is assumed to be high it may be noticed that the concentration down.

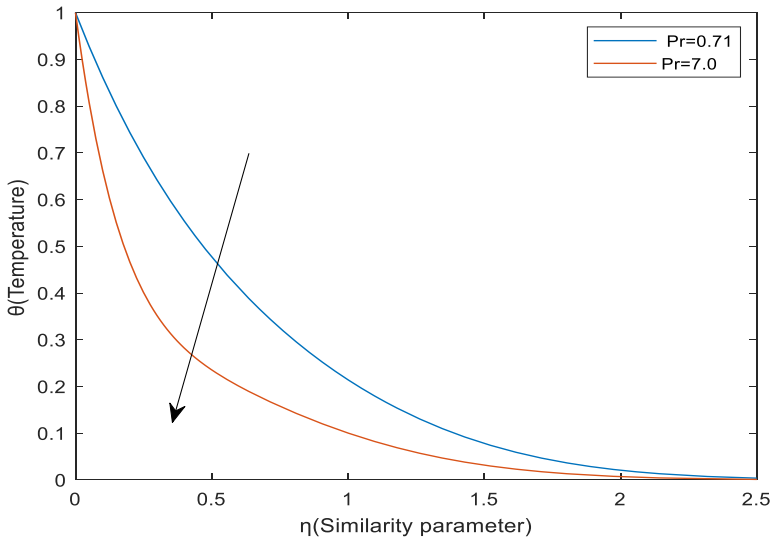

Fig .4 Temperature Profiles for several values of Pr and Sc=0.6,R=5,Q=1,K=1,Df=1,t=0.2

In Fig.4 shows that temperature decreases as in the values of pr values increases

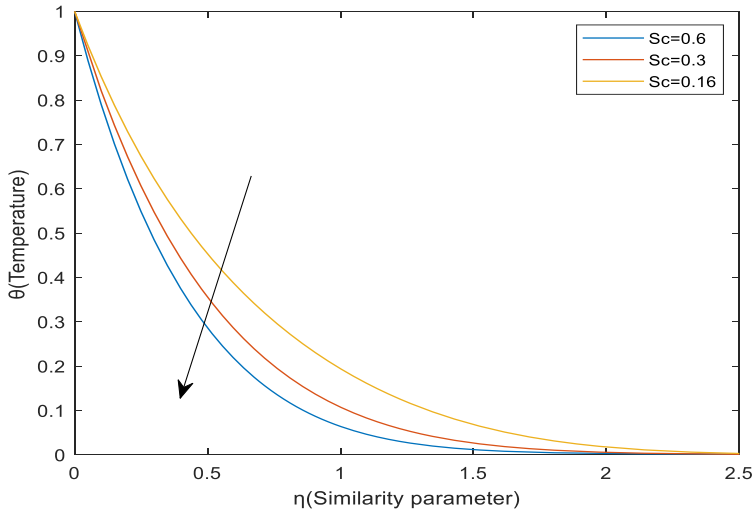

Fig.5Temperature Profiles for distinguished values of Sc and R=5,Q=1,K=1,Df=1,t=0.2,Pr=0.71

Fig.5,it is observed that Schmidt number increases, indicating a tendency for the temperature to rise initially. However, the temperature subsequently fluctuates, revealing a change in trend, decrease in warm at this stage.

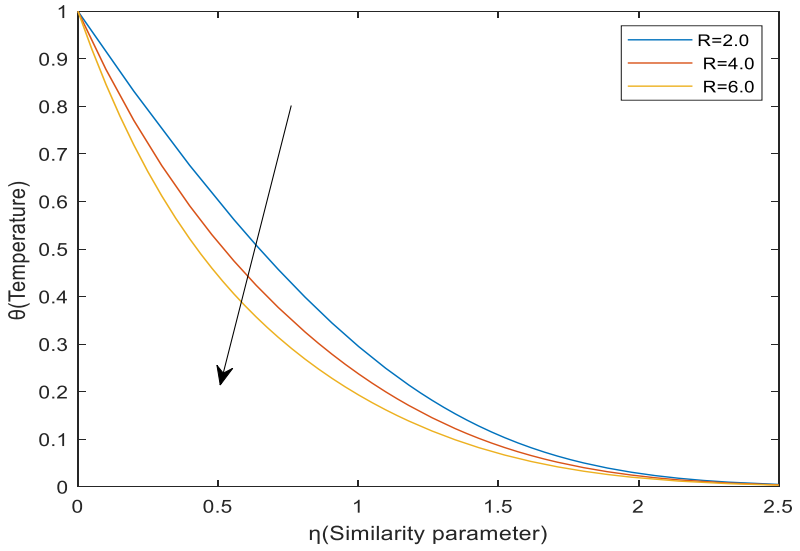

Fig.6 Temperature Profiles for several values of Chemical Reaction K and Pr=0.71, Sc=0.6,Q=1,K=1,Df=1,t=0.2

Fig. 6 illustrates the temperature profile shows that thermal radiation parameter R goes up, the temperature goes down

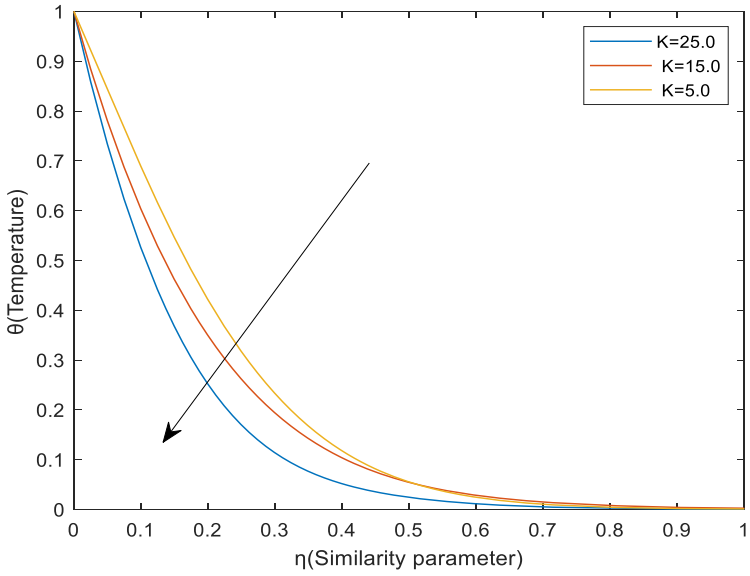

Fig.7 Temperature profiles of distinct Chemical Reaction 'K' andPr=0.71,Sc=0.6,R=2,Q=1,Df=1,t=0.2

In Fig. 7,it is observed that the chemical reaction values K goes up, then the temperature goes down

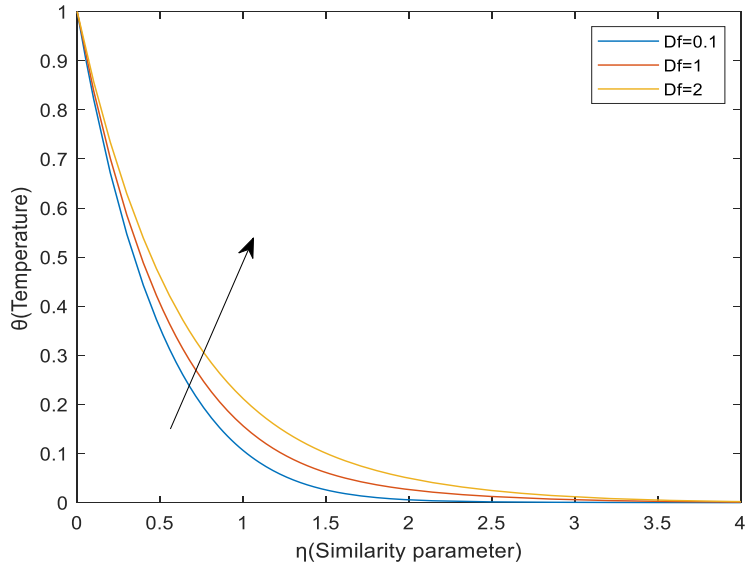

Fig.8 Temperature Profiles for various values of Df and Pr=0.71,Sc=0.6,R=6,Q=0.1,K=5,t=0.2

In Fig.8, we can explore the heat behaviour in more detailed by considering the thermal diffusion(Dufour) numbers (Df = 0.1,1,2). In general, as Dufour parameter increases, it means that the Dufour effect becomes more pronounced.

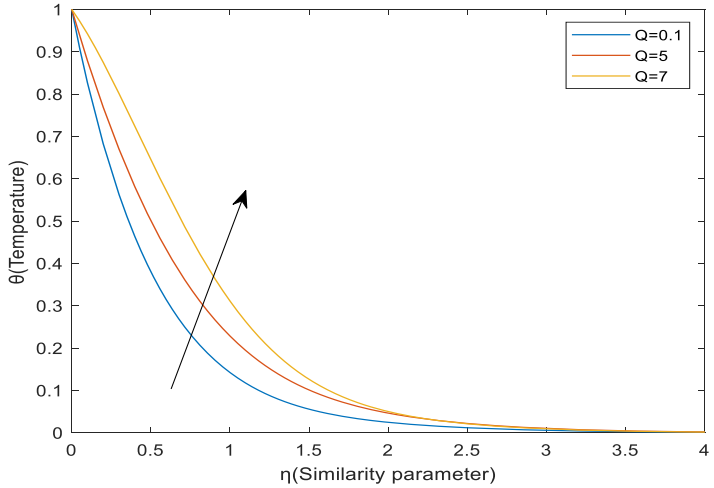

Fig.9. Temperature profile for different values of Q and Pr=0.71,Sc=0.16,R=6, K=5,Df=1, t=0.2

In Fig.9,it is observed that temperature increases with increases in the values of heat generation parameter Q

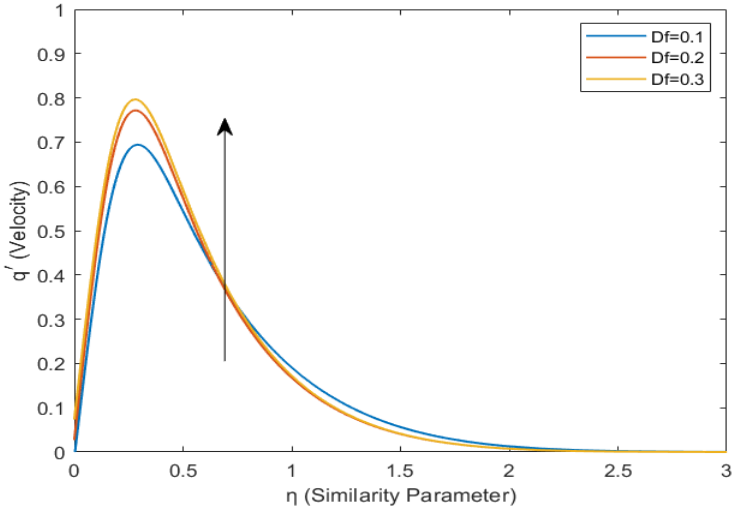

Fig.10 Velocity Profile for different values of Df and r=5,Gc=10,Pr=7,Sc=0.1,R=5,Q=1, $\gamma = 0.5$,K=0.5,Df=0.1,h=1.5,t=0.1 w=30, Ω =0.5,k1=0.4

Fig.10 illustrates speed for thermal diffusion values (Df = 0.1,0.2,0.3), it is evident that the highest speed is achieved if Dufour number gets high

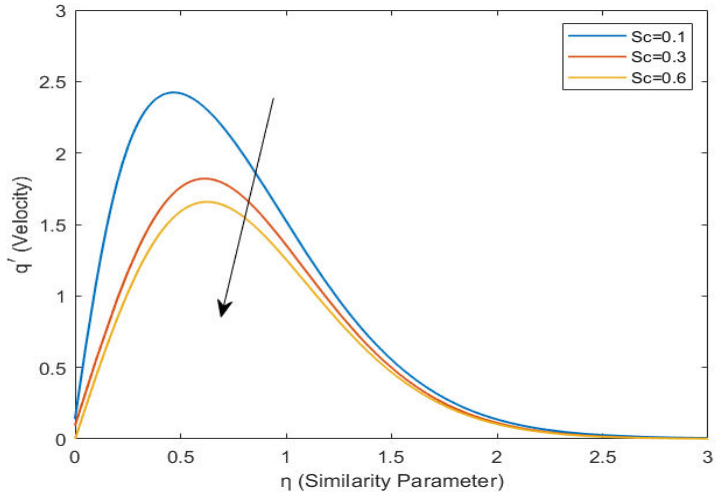

Fig. 11 Velocity for distinct values of S_c and Gr=5,Gc=10,Pr=7,R=5,Q=1, $\gamma = 0.5$,K=0.5,Df=0.1,h=1.5,t=0.1 w=30, Ω =0.5,k1=0.4

In fig.11 displays plate's velocity contours at various Schmidt values. (Sc= 0.1, 0.3, 0.6). A plate's Schmidt number falls as speed rises.

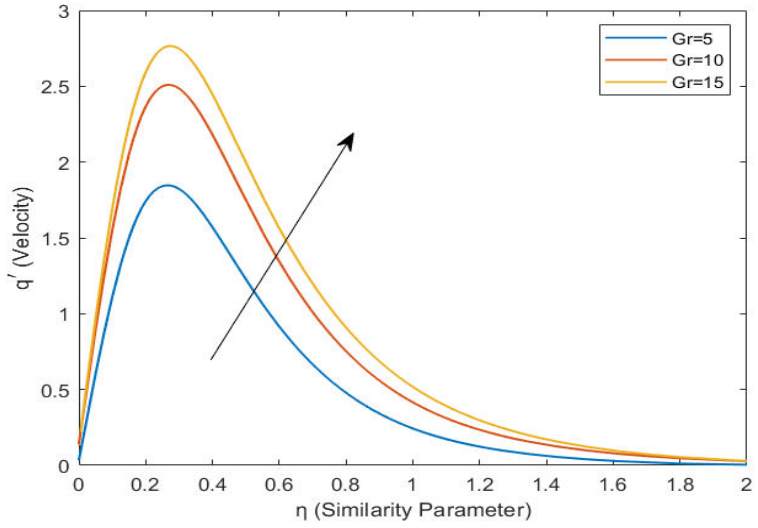

Fig.12 Velocity profile for different values of Gr and andGc=10,Pr=7,Sc=0.1,R=5,Q=1, $\gamma = 0.5$,K=0.5,Df=0.1,h=1.5,t=0.1 w=30, Ω =0.5,k1=0.4

In fig.12 velocity contours of the plate are shown in the image above. Increasing velocity causes the Gr values to increase

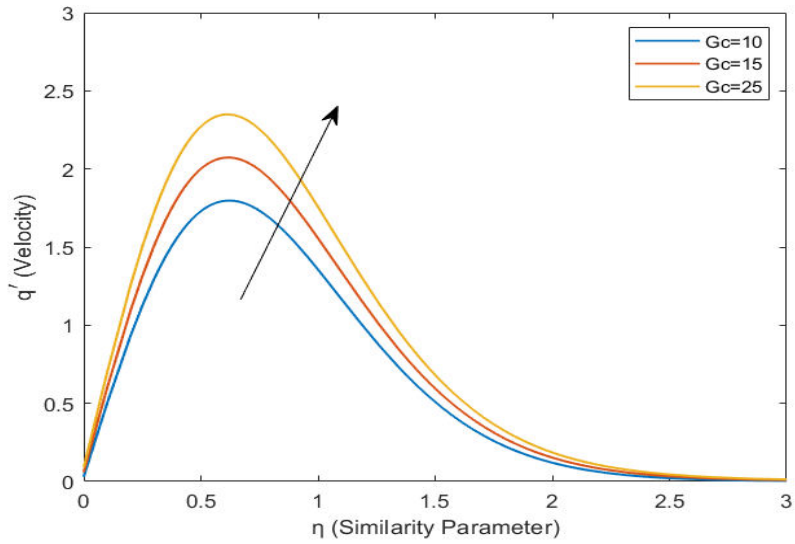

.

Fig.13 Velocity profile for different values of Gc and andGr=10,Pr=7,Sc=0.1,M=10, R=5,Q=1, $\gamma = 0.5$, K=0.5,Df=0.1,h=1.5,t=0.1 w=30, Ω =0.5,k1=0.4

In fig.13 velocity contours of the plate are shown in the image above. Increasing velocity causes the Gr values to increase.

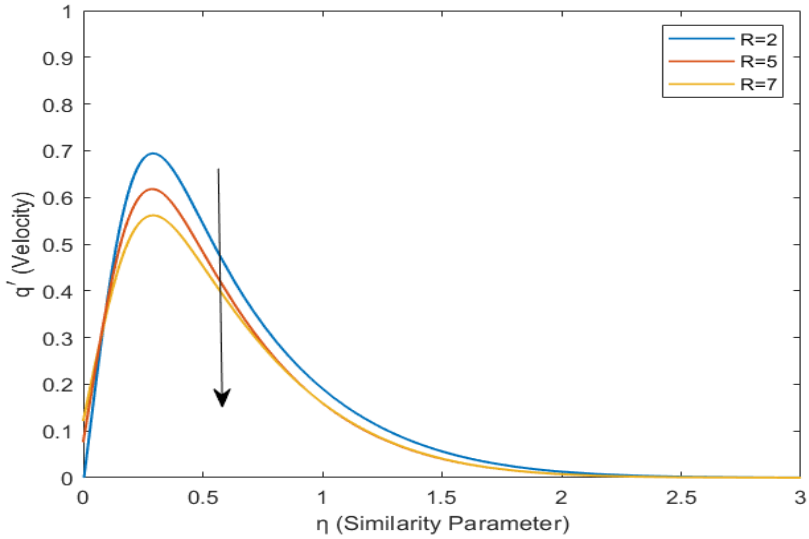

Fig.14 Velocity profile for different values of R and Gc=10,Gr=10,Pr=7,Sc=0.1, R=5,Q=1, $\gamma = 0.5$,K=0.5, Df=0.1, h=1.5, t=0.1 w=30, Ω =0.5, k1=0.4

In fig.14, it is observed that velocity of the plate goes to down with an increasing the values of thermal radiation parameter R

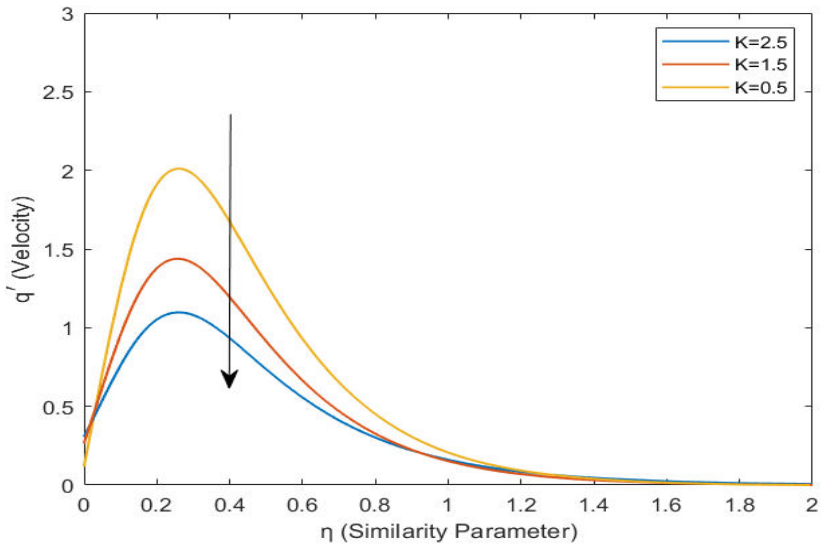

Fig.15 Velocity profile for different values of K and Gc=10,Gr=10,Pr=7,Sc=0.1, R=5,Q=1, $\gamma = 0.5$,K=0.5, Df=0.1, h=1.5, t=0.1 w=30, Ω =0.5, k1=0.4

In fig.15, it is seen that velocity of the plate goes to down with an increasing the values of chemical reaction parameter K

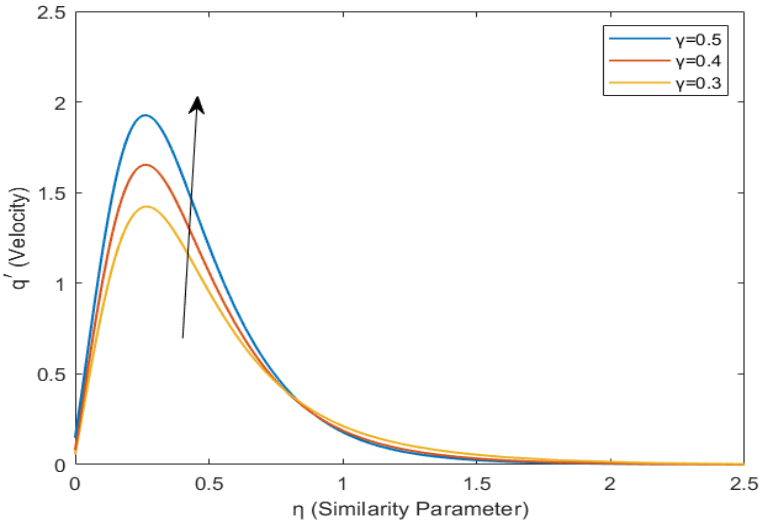

Fig.16 Velocity profile for different values of γ and Gc=10,Gr=10,Pr=7,Sc=0.1,R=5, Q=1, K=0.5, Df=0.1, h=1.5, t=0.1 w=30, Ω =0.5, k1=0.4

In fig.16, it is seen that velocity of the plate goes to high performance with an increasing the values of Casson fluid parameter

5. Conclusion

This research explores the relationship between rotational and Dufour effects on Casson fluid flow, using Laplace transforms to understand equations and mathematical statements.

Graphs display findings, highlighting temperature, concentration, and speed schemes.

- The temperature profile tends to increase in the Dufour number (Df), heat generation (Q), and time (t), and experiences a reversal in the Prandtl number (Pr), Schmidt number (Sc), chemical reaction parameter (K), and thermal radiation parameter (R).
- The concentration boundary layer decreased and reversed on time (t) as the Schmidt number (Sc) and chemical reaction parameter (K) rose.
- The speed slows down and the Defour number goes up as the values of the thermal gradient number (Gr), the Casson fluid parameter (γ), the chemical reaction parameter (K), the Schmidt number (Sc), the thermal radiation parameter (R), and the Prandtl number (Pr) go up.

References

1. Muthucumaraswamy, R., and J. Venkatesan. "Radiative flow past a parabolic started isothermal Vertical plate with uniform mass flux." *International Journal of Mathematical Analysis* 7 (2013): 2907-2921.
2. A.K. Agrawal, S.N. Gupta and N.K. Samria, Study of heat and mass transfer past a parabolic started infinite vertical plate, Journal of Heat and mass transfer, 21 (1999), 67 – 75.
3. Kataria, Hari R., and Harshad R. Patel. "Radiation and chemical reaction effects on MHD Casson fluid flow past an oscillating vertical plate embedded in porous medium." *Alexandria Engineering Journal* 55, no. 1 (2016): 583-595.
4. Vijayaragavan, R., M. Ramesh, and S. Karthikeyan. "Heat and Mass Transfer Investigation on MHD Casson Fluid Flow past an Inclined Porous Plate in the Effects of Dufour and Chemical Reaction." *Journal of Xi'an University of Architecture and Technology* 13 (2021): 860-873.
5. Kavitha, S., Ayothi Selvaraj, Senthamilselvi Sathiamoorthy, and P. Rajesh. "A Parabolic Flow with MHD, the Dufour and Rotational Effects of Uniform Temperature and Mass Diffusion through an Accelerating Vertical Plate in the Presence of Chemical Reaction." *Journal of Advanced Research in Fluid Mechanics and Thermal Sciences* 110, no. 2 (2023): 192-205.
6. Selvaraj, A., S. Dilip Jose, R. Muthucumaraswamy, and S. Karthikeyan. "MHD-parabolic flow past an accelerated isothermal vertical plate with heat and mass diffusion in the presence of rotation." Materials Today: Proceedings 46 (2021): 3546-3549. https://doi.org/10.1016/j.matpr.2020.12.499
7. Nandakumar, V., S. Senthamilselvi, and Ayothi Selvaraj. "Soret and MHD Effects of Parabolic Flow Past through an Accelerated Vertical Plate with Constant Heat and Mass Diffusion in the Presence of Rotation, Chemical Reaction and Thermal Radiation." *Journal of Advanced Research in Fluid Mechanics and Thermal Sciences* 112, no. 1 (2023): 125-138.
8. Selvaraj A., Jothi. 'Heat source impacts on MHD and radiation absorption fluid flow past an exponentially accelerated vertical plate with exponentially variable temperature and mass diffusion through porous medium.' Materials Today proceeding 46, no.9: 3590-3594. https://doi.org/10.1016/j.matpr.2020.11.919
9. Lakshmikaanth D., A.Selvaraj , P.Selvaraju and S. Dilip Jose. 'Hall and Heat Source Effects of Flow Past a Parabolic Accelerated Isothermal Vertical Plate in The Presence Of Chemical Reaction And Radiation.' JP Journal of Heat and Mass Transfer 34,(2023):105-126.https://doi.org/10.17654/0973576323035
10. Maran D., Selvaraj A., Usha M., Dilipjose. 'First order chemical response impact of MHD flow past an infinite vertical plate with in the sight of exponentially with variable mass diffusion and thermal radiation.' Materials Today: Proceedings 46, (2021): 3302-3307. https://doi.org/10.1016/j.matpr.2020.11.464

11. Aruna, M., A. Selvaraj, and V. Rekha. "Hall and Magnetic Impacts on Stream Past a Parabolic Accelerated Vertical Plate with Varying Heat and Uniform Mass Diffusion in the Appearance of Thermal Radiation." In *International Conference on Advancement in Manufacturing Engineering*, pp. 323-336. Singapore: Springer Nature Singapore, 2022.
12. Radha, Ganesan, Ayothi Selvaraj, Soundararajan Bhavani, and Periasamy Selvaraju. "Magneto Hydrodynamic Effects on Unsteady Free Convection Casson Fluid Flow Past on Parabolic Accelerated Vertical Plate with Thermal Diffusion." *Journal of Advanced Research in Fluid Mechanics and Thermal Sciences* 116, no. 1 (2024): 184-200.
13. Muthukumaraswamy, R., and P. Ganesan. "Unsteady flow past an impulsively started vertical plate with heat and mass transfer." *Heat and Mass transfer* 34, no. 2 (1998): 187-193.
14. Muthucumaraswamy, R., M. Thamizhsudar, and J. Pandurangan. "Hall Effects On MHD Flow Past An Exponentially Accelerated Vertical Plate In The Presence Of Rotation." *Annals of the Faculty of Engineering Hunedoara* 12, no. 3 (2014): 145.
15. R.B.HetnarskizastosowaniaMatematyki VII (1964).On inverting the Laplace Transformsconnected with the error function. Applications Mathematica,Vol:7, no 4, pp:399-40.
16. R.B.Hetnarski (1975): An algorithm for generating some inverse Laplace transform of exponential formZAMP Vol 26 , pp:249-253. https://doi.org/10.1007/bf01591514.
17. Sarma, Subhrajit, and Nazibuddin Ahmed. "Dufour effect on unsteady MHD flow past a vertical plate embedded in porous medium with ramped temperature." *Scientific Reports* 12, no. 1 (2022): 13343.
18. J Prakash A Selvaraj, "Effects of Radiation and Heat Generation on MHD and Parabolic Motion on Casson Fluids Flow Through a Rotating Porous Medium in a Vertical Plate", J. Appl. Math. & Informatics Vol. 42(2024), No. 3, pp. 607 - 623
19. Reddy, B. Prabhakar, O. D. Makinde, and Alfred Hugo. "A computational study on diffusion-thermo and rotation effects on heat generated mixed convection flow of MHD Casson fluid past an oscillating porous plate." *International Communications in Heat and Mass Transfer* 138 (2022): 106389.
20. Reddy, N. Ananda, and K. Janardhan. "Soret and Dufour effects on MHD Casson fluid over a vertical plate in presence of chemical reaction and radiation." *Int. J. Curr. Res. Rev* 9, no. 24 (2017): 55-61.
21. Palani, G., and A. Arutchelvi A. Arutchelvi. "MHD Nanofluid Flow Past an Inclined Plate with Soret and Dufour Effects." *Jp Journal of Heat and Mass Transfer* 31 (2023): 123-145.
22. Kumar MA, Reddy YD. Combined effects of chemical reaction, Dufour, Soret effects on unsteady MHD flow past an impulsively started inclined porous plate with variable temperature and mass diffusion. Int. J. Math. Archive. 2016;7(9):98-111.
23. Vempati SR, Laxmi-Narayana-Gari AB. Soret and Dufour effects on unsteady MHD flow past an infinite vertical porous plate with thermal radiation. Applied Mathematics and Mechanics. 2010 Dec;31:1481-96. https://doi.org/10.1007/s10483-010-1378-9
24. Muthucumaraswamy R, Radhakrishnan M. Chemical reaction effects on flow past an accelerated vertical plate with variable temperature and mass diffusion in the presence of magnetic field. Journal of Mechanical Engineering and Sciences. 2012 Dec 31;3:251-60. https://doi.org/10.15282/jmes.3.2012.1.0023
25. Muthucumaraswamy R, Dhanasekar N, Prasad GE. Mass transfer effects on accelerated vertical plate in a rotating fluid with first order chemical reaction. Journal of Mechanical Engineering and Sciences. 2012 Dec 31;3:346-55. https://doi.org/10.15282/jmes.3.2012.11.0033

26. Patel, Harshad R. "Effects of cross diffusion and heat generation on mixed convective MHD flow of Casson fluid through porous medium with non-linear thermal radiation." *Heliyon* 5, no. 4 (2019).
27. Dhanalakshmi, E., P. Rajesh, P. Kandan, M. Kesavan, G. Jayaraman, A. Selvaraj, and R. Priya. "Stability of bonds, kinetic stability, energy parameters, spectral characterization, GC–MS and molecular descriptors studies on coumarine, 3-[2-(1-methyl-2-imidazolylthio)-1-oxoethyl]." *Journal of Molecular Structure* 1295 (2024): 136544
28. Karthikeyan, S., A. Selvaraj, and M. Venkateswarlu. "Rotating significance of parabolical movement antique with an appearance on isothermal vertical plate by MHD." *Materials Today: Proceedings* (2021
29. Karthikeyan, S., and A. Selvaraj. "Uniform mass diffusion on thermal radiation with rotation of parabolic in progress vertical plate set MHD." *Materials Today: Proceedings* (2021
30. Gayathri, M., B. Hari Babu, and M. Veera Krishna. "Soret and Dofour effects on unsteady MHD convection flow over an infinite vertical porous plate." *Modern Physics Letters B* (2024): 2450449Ramesh, M., Palanikumar, K., & Reddy, K.H. (2013). Mechanical property evaluation of sisal-jute-glass fiber reinforced polyester composites. Composites Part B: Engineering, 48, 1-9.